



Published in final edited form as:

Nature. 2015 July 23; 523(7561): 477–480. doi:10.1038/nature14651.

## Genetic modification of the diarrheal pathogen *Cryptosporidium parvum*

Sumiti Vinayak<sup>1,\*</sup>, Mattie C. Pawlowic<sup>1,\*</sup>, Adam Sateriale<sup>1,\*</sup>, Carrie F. Brooks<sup>1</sup>, Caleb J. Studstill<sup>1</sup>, Yael Bar-Peled<sup>1</sup>, Michael J. Cipriano<sup>1</sup>, and Boris Striepen<sup>1,2,†</sup>

<sup>1</sup>Center for Tropical and Emerging Global Diseases, University of Georgia, Paul D. Coverdell Center, 500 D.W. Brooks Drive, Athens, GA 30602, U.S.A

<sup>2</sup>Department of Cellular Biology, University of Georgia, Paul D. Coverdell Center, 500 D.W. Brooks Drive, Athens, GA 30602, U.S.A

### Abstract

Recent studies into the global causes of severe diarrhea in young children have identified the protozoan parasite *Cryptosporidium* as the second most important diarrheal pathogen after rotavirus<sup>1–3</sup>. Diarrheal disease is estimated to be responsible for 10.5% of overall child mortality<sup>4</sup>. *Cryptosporidium* is also an opportunistic pathogen in the context of HIV-AIDS and organ transplantation<sup>5,6</sup>. There is no vaccine and only a single approved drug that provides no benefit for those in gravest danger, malnourished children and immunocompromised patients<sup>7,8</sup>. *Cryptosporidiosis* drug and vaccine development is limited by the poor tractability of the parasite, which includes lack of continuous culture, facile animal models, and molecular genetic tools<sup>3,9</sup>. Here we describe an experimental framework to genetically modify this important human pathogen. We establish and optimize transfection of *C. parvum* sporozoites in tissue culture. To isolate stable transgenics we develop a mouse model that delivers sporozoites directly into the intestine, a *Cryptosporidium* CRISPR/Cas9 system, and *in vivo* selection for aminoglycoside resistance. We derive reporter parasites suitable for *in vitro* and *in vivo* drug screening, and we evaluate the basis of drug susceptibility by gene knock out. We anticipate the ability to genetically engineer the parasite will be transformative for *Cryptosporidium* research. Genetic reporters will provide quantitative correlates for disease, cure and protection and the role of parasite genes in these processes is now open to rigorous investigation.

Reprints and permissions information is available at [www.nature.com/reprints](http://www.nature.com/reprints).

<sup>†</sup>To whom correspondence should be addressed: Tel.: 1-706-583-0588; Fax: 1-706-542-3582; [striepen@uga.edu](mailto:striepen@uga.edu).

\*These authors contributed equally to this study

### Competing Financial Interests

SV, CFB and BS are listed as inventors on the Patent Cooperation Treaty (PCT) application entitle *Cryptosporidium* transfection methods and transfected *Cryptosporidium* cells filed by the University of Georgia Research Foundation.

### Author Contributions

SV developed transfection and luciferase assay; MCP optimized transfection and developed Cas9 system; SV, MCP, AS, CFB developed mouse infection and AS developed selection assays; CFB developed surgery; CJS and YBP constructed some of the plasmids; and MJC provided bioinformatics support. SV, MCP, AS and CFB conducted animal experiments and genotypic and phenotypic characterization. SV, MCP, AS, CFB and BS conceived of the study and BS wrote the manuscript with contributions from SV, MCP and AS.

*Cryptosporidium* infection occurs through fecal oral transmission of the environmentally resilient oocyst. The oocyst shelters four sporozoites that emerge in the small intestine and invade the epithelium. While there is no tissue culture system for continuous passage, *Cryptosporidium parvum* development can be observed for 2–3 days by infecting human ileocecal adenocarcinoma cells (HCT-8)<sup>10</sup>. To achieve transfection sporozoites were excysted from oocysts purified from the feces of experimentally infected calves using a protocol that mimics stomach and intestinal passage<sup>11</sup>, and then electroporated prior to infection of HCT-8 cells (Fig. 1a). The transfection plasmids used here flanked a variety of reporter genes with candidate *C. parvum* 5' and 3' regulatory sequences derived from highly expressed housekeeping genes. We observed significant reporter activity 48 hours after transfection using plasmids carrying nanoluciferase (Nluc, Fig. 1b), a small ATP independent enzyme from deep sea shrimp<sup>12</sup>, but not firefly luciferase or fluorescent proteins. Nluc luminescence correlated with the number of parasites and the amount of DNA used for transfection. Luminescence was also shown to require the presence of parasite specific promoter elements and the introduction of DNA into parasites and not host cells (Fig. 1). Furthermore, reporter signal was ablated by the antiparasitic drug nitazoxanide. Transient transfection of *C. parvum* is inefficient (<10,000 fold when compared to the related apicomplexan *Toxoplasma gondii* in parallel experiments) and requires a highly sensitive reporter like Nluc to be noticeable.

In an effort to enhance efficiency we evaluated different electroporation devices, electrical wave programs, and buffer compositions (Extended Data Fig. 1), this produced tenfold enhancement. We tested flanking sequences from different *C. parvum* genes and identified the enolase promoter to be strongest. The *C. parvum* genome is AT rich and shows significant codon bias<sup>13</sup>, we also noted preference of A over T within the first 20 codons and thus explored codon optimization and found sixfold enhancement (Fig. 1j).

To enable enrichment of transgenic parasites we next explored selection of drug resistance. The aminoglycoside antibiotic paromomycin does not cure cryptosporidiosis in people, but is effective in tissue culture (Fig. 2a) and in immunocompromised mice<sup>14</sup>. Work in other protist models has shown aminoglycoside phosphotransferases to confer resistance to paromomycin<sup>15,16</sup>. Appreciation of *C. parvum* drug resistance in culture is complicated by the lack of continuous growth. We thus constructed translational fusions between the Nluc reporter and the neomycin resistance marker (Neo)<sup>15</sup> to focus our observation on the small subset of transfected parasites. Luciferase activity in parasites expressing Nluc-Neo showed reduced susceptibility to paromomycin treatment compared to Nluc alone (Fig. 2c), and thus we concluded that Nluc-Neo confers drug resistance in this transient assay.

Our genome searches indicated that *Cryptosporidium* species lack nonhomologous end joining DNA repair. This suggested transgene integration to be rare and to require homologous recombination<sup>17,18</sup>. Such recombination can be enhanced by long flanking regions and/or double strand breaks introduced by restriction enzymes, TALENs or CRISPR/Cas9<sup>18,19</sup>. To build a *C. parvum* CRISPR/Cas9 system we constructed a plasmid where the *C. parvum* U6 RNA promoter drives a guide RNA cassette<sup>20</sup> and the *Streptococcus pyogenes* Cas9 gene<sup>21</sup> is flanked by parasite regulatory sequences (Fig. 2d). To test this system we conducted a Cas9 dependent DNA repair experiment (Fig. 2e–g). We

introduced a stop codon into the Nluc reporter that ablated luciferase activity (**Dead Nluc**). We then targeted the dead gene with a guide RNA, and provided a short double-stranded template for repair that restores read through translation and renders the repaired gene resistant to further Cas9 cutting. When *C. parvum* sporozoites are cotransfected with a specific guide, luciferase activity is restored ( $p=0.0006$ , unpaired *t* test). No change is observed with no or off target guides.

Interferon gamma knockout mice are susceptible to *C. parvum* infection through oral inoculation of oocysts<sup>22</sup>. However, infection with free sporozoites is less effective<sup>23</sup>, likely due to stomach passage. We developed a surgical protocol to inject transfected sporozoites directly into the small intestine to maximize infection (Extended Data Fig. 2). When mice were sacrificed 24 hours after infection luciferase activity was observed in scrapings of the intestinal epithelium. We also established an effective treatment protocol using paromomycin supplementation of the drinking water (Extended Data Fig. 3).

Next we infected mice by surgery with transfected sporozoites and treated with paromomycin as indicated (Fig. 3 and Extended Data Fig. 4, four mice per group). Feces were collected every three days and oocyst shedding was measured by quantitative PCR targeting the *C. parvum* 18S ribosomal RNA locus. Mice infected with parasites transfected with the **Nluc-Neo** plasmid that did not receive drug shed high numbers of oocysts and remained infected for the 30 days observed (Fig. 3b, blue). Those infected with parasites that received the **Nluc** plasmid (lacking the Neo gene, green) were rapidly cured by drug treatment. Those transfected with **Nluc-Neo** alone and drug treated were also cured (infection may persist slightly longer). In contrast, infection with parasites carrying the **Nluc-Neo** plasmid and the **Cas9** plasmid (red, Cas9 target detailed below) rapidly rebounded to levels similar to untreated mice. Oocysts emerging from selection were purified from feces and used to infect mice that were again treated with paromomycin, wild type oocyst were used in parallel (100,000 oocysts per mouse by gavage). While paromomycin treatment cured infection with wild type parasites, transgenic parasites showed immediate robust drug resistance (Fig. 3c). When these oocysts were probed by Western blot with anti Neo antibody we detected a band consistent with an Nluc-Neo fusion protein.

Purified oocysts were also used to infect cell cultures, and processed for immunofluorescence after 2 days. Transgenic but not wild type intracellular parasite stages showed fluorescence when probed with antibodies specific for either Neo or Nluc (Fig. 2e). These cultures also displayed strong luciferase activity not observed in wild type. This activity exceeded that previously observed in transient transfection experiments by five orders of magnitude on a per cell basis. We assessed whether these organisms may be suitable for drug screening assays by infecting 96 well plates with 1,000 oocyst per well and measured luciferase after 48h. Infected wells are clearly distinguished from uninfected ( $z' > 0.6$ ,  $n=20$ ). Similarly, wells treated with nitazoxanide showed significant growth inhibition ( $p=0.0036$ , unpaired *t* test). Luciferase also provided a faster way to assess the infection state of animals. We sampled 10 mg of feces from mice diagnosed in parallel by PCR and found this assay to be sensitive and specific (Fig. 3d). We note that Nluc expression remains stable

when parasites are propagated in mice in the absence of paromomycin (Extended Data Fig. 5).

*Cryptosporidium* is remarkably resistant to antifolates, a mainstay of treatment against other apicomplexans, and this resistance has been attributed to differences in the target enzyme dihydrofolate reductase-thymidylate synthase (DHFR-TS)<sup>24</sup>. However, *Cryptosporidium* is unique among apicomplexans in that it acquired a thymidine kinase (TK) by horizontal gene transfer from bacteria<sup>25</sup>. We hypothesized that TK may also contribute to *Cryptosporidium* antifolate resistance by providing an alternative route to dTMP (Fig. 4a). For this reason the TK locus was targeted for insertion, allowing us to test this hypothesis by gene disruption. We mapped the locus in stable transgenic parasites by PCR using primers that link the marker genes with genomic sequences beyond the flanking regions on the targeting construct. This mapping is consistent with insertion by homologous double crossover (Fig. 4b,c). Furthermore, the TK coding sequence is no longer detectable indicating uniform loss of the gene in the selected population. We tested for DNA incorporation of the thymidine analog 5-ethynyl-2'-deoxyuridine (EdU) using click chemistry and fluorescence microscopy<sup>26</sup>. Wild type parasites grown in the presence of EdU show fluorescent nuclei. This labelling is lost in the transgenic (Fig. 4d, e) confirming loss of TK at the biochemical level. We next treated with the antifolate trimethoprim. We confirmed the previously observed resistance in wild type parasites, but noted enhanced susceptibility in the mutant (Fig. 4f). We conclude that the *C. parvum* TK gene is a non-essential enzyme required for the activation of thymidine, and that its presence limits the efficacy of antifolate therapy in *Cryptosporidium*.

In summary, we show that significant hurdles towards genetic analysis and manipulation for cryptosporidiosis can be overcome by maximizing the efficiency of each step of the process and by focusing on *in vivo* propagation and selection. There is urgent need for new anti-parasitic drugs<sup>3</sup>. *Cryptosporidium* is not susceptible to drugs widely used against related pathogens, which reflects substantial differences in metabolism and uptake<sup>27</sup>. Luciferase reporter parasites enable phenotypic screening in culture and animals with sufficient sensitivity and specificity to warrant a comprehensive effort to discover novel compounds. Gene deletion now permits biological target validation. Genetic modification may also allow the construction of attenuated parasites as a potential oral vaccine. While infants and toddlers are highly susceptible to the disease, infection is rarely detected in older children<sup>1,3</sup>. This is consistent with infection studies in people and animals in suggesting the development of anti-parasitic and anti-disease immunity<sup>3,28,29</sup>. A better understanding of the mechanisms underlying disease and protection will be required to design and produce such a vaccine.

## Methods

### *C. parvum* reporter and drug resistance vectors

*C. parvum* transfection vectors were derived from plasmid pH3BG<sup>19</sup> and modified to contain *C. parvum* promoter and 5' and 3' untranslated mRNA regions. We mined the genome and a variety of expression data sets collectively available through [cryptoDB.org](http://cryptoDB.org)<sup>31</sup> to identify genes that are highly expressed across the lifecycle. Promoters and 5'UTRs of the

enolase (cgd5\_1960),  $\alpha$ -tubulin (cgd4\_2860), and aldolase (cgd1\_3020) genes and 3' UTRs of enolase (51 bp),  $\alpha$ -tubulin (97 bp), or ribosomal protein L13A (cgd5\_970, UTR 211 bp) were amplified from genomic DNA by PCR (see Table S1 for a list of primer sequences and restriction sites used). Nluc was amplified from pNL1.1 (Promega Corporation, Madison, WI), firefly luciferase and different fluorescent protein genes were amplified from vectors used for *T. gondii*<sup>32–34</sup>. The neomycin resistance gene was amplified from plasmid pNeo4<sup>15</sup> (a kind gift of Jacek Gaertig, University of Georgia, Athens, GA) and introduced 5' or 3' of Nluc in a plasmid with enolase regulatory sequences. To target the TK gene, regions flanking the gene were amplified and introduced into the Nluc-Neo vector (the promoter but not the 3' UTR were retained).

### ***C. parvum* CRISPR/Cas9 genome editing**

Human codon-optimized *Streptococcus pyogenes* Cas9 (hSpCas9) carrying a FLAG tag and N- and C-terminal nuclear localization signals was amplified from pX330<sup>35</sup> and introduced into the Aldolase-Nluc-ribo vector replacing the Nluc. A guide RNA cassette was synthesized containing the *C. parvum* U6 promoter identified by genome searches using known structural RNA sequences from *P. falciparum*<sup>36</sup>, two inverted BbsI restriction sites to facilitate guide cloning, a trans-activating CRISPR RNA (tracrRNA) consensus sequence and a terminator (poly T) sequence, and was introduced into the Cas9 plasmid.

To test for CRISPR/Cas9 mediated repair *in vitro*, we modified the codon optimized Nluc vector by introducing a premature stop codon (Y18Stop) adjacent to a guide target sequence at the beginning of the gene by site-directed mutagenesis (QuikChange II, Agilent Technologies, Santa Clara, CA). A 125 bp dsDNA oligonucleotide was synthesized that restored Y18 and disrupted the PAM-motif (G17A) of the guide RNA target thus rendering it resistant to further Cas9 cuts.

### **Parasite excystation and transfection**

Oocyst excystation was carried out as described<sup>11</sup> with some modification. Up to 10<sup>8</sup> *C. parvum* Iowa strain oocysts (Sterling Parasitology Laboratory, University of Arizona, Tucson, AZ or Bunch Grass Farm, Deary, ID) were suspended in 100  $\mu$ l of 1:4 aqueous dilution of 5.25% sodium hypochlorite and incubated on ice for 5 min. Oocysts were then washed three times with ice-cold phosphate-buffered saline (PBS), suspended at 3.9 $\times$ 10<sup>5</sup> oocysts/ml of 0.2 mM sodium taurocholate (prepared in PBS) and incubated at 15°C (10 min) and then at 37°C (60–90 min). Emergence of sporozoites was monitored microscopically (typical efficiency 70–90%). Sporozoites were filtered through a 3  $\mu$ m polycarbonate filter to remove unexcysted oocysts, washed with ice-cold PBS, and counted.

Initially we used a BTX ECM 630 device for electroporation (Harvard Apparatus, Inc., Holliston, MA). Excysted sporozoites (10<sup>7</sup>) were suspended in complete cytomix buffer (120 mM KCl, 0.15 mM CaCl<sub>2</sub>, 10 mM K<sub>2</sub>HPO<sub>4</sub>/KH<sub>2</sub>PO<sub>4</sub>, pH 7.6, 25 mM HEPES, pH 7.6, 2 mM EGTA, 5 mM MgCl<sub>2</sub>, pH 7.6 supplemented with 2 mM ATP and 5 mM glutathione), mixed with plasmid DNA, and electroporated with a single 1500V pulse, resistance of 25  $\Omega$ , and a capacitance of 25  $\mu$ F. To enhance transfection efficiency, we switched to using the AMAXA Nucleofactor 4D device (Lonza Cologne GmbH, Cologne, Germany). After

excystation  $10^7$  sporozoites were suspended in 15  $\mu$ l Lonza SF Buffer and combined with 10–50  $\mu$ g DNA (prepared in Tris-EDTA, pH 8.0) at a final volume of 20  $\mu$ l. The parasite-DNA mix was added to small, strip cuvettes and electroporated using program EH100. Additional electroporation conditions were explored to arrive at this protocol and those are listed in Extended Data Fig. 1.

For *in vitro* transfection assays, human ileocecal colorectal adenocarcinoma (HCT-8) cells (ATCC, Manassas, VA) were grown in RPMI-1640 with glutamine supplemented with 10% FBS, 1 mM sodium pyruvate, 50 U/ml penicillin, 50  $\mu$ g/ml streptomycin and amphotericin B in 24, 48, or 96 well plates to 70% confluency. No effort was made to authenticate this cell line or test for mycoplasma. Prior to infection, media was replaced with DMEM with 2% FBS, 50 U/ml penicillin, 50  $\mu$ g/ml streptomycin and amphotericin B, and 0.2 mM L-glutamine. For *in vivo* experiments electroporated sporozoites were suspended in PBS and kept on ice until administered to the mice.

The *T. gondii* Nluc plasmid was constructed by inserting the Nluc sequence into pCTH<sub>3</sub> vector<sup>32</sup> and parasites were electroporated and used to infect human foreskin fibroblasts as described<sup>37</sup>. HCT-8 cells were cultured in 24 well plates until confluent, transfected with 500 ng of DNA using Lipofectamine 2000 as described by the manufacturer (Life Technologies), and assayed for Nluc activity after 48 hours.

### Animal ethics statement

Animal experiments were approved by the Institutional Animal Care and Use Committee of the University of Georgia (animal use protocol # A2012 03-028-Y3-A12).

### Surgical delivery of transfected sporozoites into IFN-gamma deficient mice

In preliminary experiments we noted that antibiotic removal of bacterial flora enhances susceptibility of mice. Prior to infection mice were orally treated by gavage daily for a week prior to infection with an antibiotic cocktail (3mg ampicillin, 3mg streptomycin, 0.95mg metronidazole, 3mg neomycin, and 1.5mg vancomycin in dH<sub>2</sub>O, per mouse/per day, all antibiotics purchased from Sigma). To deliver sporozoites directly to the small intestine, we developed a mouse survival surgery protocol for female C57BL/6 IFN- $\gamma$  deficient mice (B6.129S7-Ifng<sup>tm1Ts</sup>/J, Jackson Laboratories, Bar Harbor, ME) aged 6–8 weeks. The abdominal area of mice was shaved with clippers. Animals were placed in isoflurane (3–5%) anesthesia induction chamber and then moved to a nosecone (1–3% isoflurane as needed) on a sterile surgical field. A sterile drape was applied over a warming pad after sterilization of the area with 70% ethanol. Respiration and response to stimulation (toe pinch) was monitored during the procedure and the vaporizer adjusted as needed. Mucous membranes and footpads were monitored for color to confirm adequate perfusion. Three betadine (Povidone-iodine) scrubs followed by a 70% ethanol wipe were applied to shaved skin prior to surgery. Ophthalmic ointment (Puralube®, Dechra Veterinary Products, Shrewsbury, UK) was applied to prevent drying of eyes. Skin was vertically incised midline of the abdominal region below the sternum with microsurgical scissors for approximately 1.5 cm followed by vertical incision of the peritoneum. Exposed jejunum/ileum was injected with  $10^7$  transfected sporozoites suspended in 200 $\mu$ l PBS containing sterile food coloring

dye as tracer. After injection, suturing was performed to close the peritoneum. Mice were administered 0.01–0.02 ml/gram body weight of warm lactated Ringer's solution subcutaneously after surgery. Meloxicam analgesic was also administered to the mice post surgery. At completion of procedure, the eye ointment was wiped off and the vaporizer was turned off and the mice were allowed to breathe the oxygen supply gas until they began to wake. Mice were placed in a recovery area until ambulatory and exhibiting normal respiration and were watched for 2 hours post surgery. Incision sites were monitored daily until fully healed (10–14 days). 24 hours following surgical infection, water in mouse cages was replaced with dH<sub>2</sub>O containing 16 mg/ml paromomycin, a concentration we determined to deliver a daily dose of 40 mg/kg paromomycin to each mouse (Extended Data Fig. 3). Mice were randomly assigned to groups before surgery. A sample size of 4 animals per treatment group was judged to be sufficiently large enough to draw appropriate conclusions. All mice survived surgery and were included in the results reported here. Investigators were not blinded to group allocation during the experiments.

### Mouse feces collection and storage

Fecal samples were collected from mice (typically 4 mice per cage) starting three days post infection every third day for up to a month. Mice were transferred to a fresh, sterile cage for 2–3 hours, and feces from the cage were collected, pooled, and stored at 4°C.

### Luciferase assay

For transient transfection experiments, electroporated sporozoites were added to 70% confluent HCT-8 culture and infection was allowed to proceed at 37°C for 48 hours. Media was removed from wells and 200 µl of lysis buffer (50mM TrisHCl, 10% glycerol, 1% Triton-X, 2mM DTT, 2mM EDTA) supplemented with NanoGlo substrate (1:50, Promega Corp., Madison, WI) was added to each well. Cells were scraped and the lysate was transferred to white 96 well plates and luminescence was measured using a Synergy H4 Hybrid Microplate Reader (BioTek Instruments, Inc., Winooski, VT). For drug assays with purified stable transgenic oocysts, the culture supernatant was collected after 48 hours from 96 well plates. An equal amount of supernatant and NanoGlo lysis buffer with substrate was combined and luminescence was measured.

For luciferase measurement from mouse fecal samples, 20 mg of feces was weighed into a 1.5 ml microcentrifuge tube and homogenized in 1 ml of lysis buffer (see above) using 10–15 glass beads (3mm) and a vortex mixer for 1 min, followed by clarification of lysate by brief centrifugation. 100 µl lysate was mixed with an equal volume of NanoGlo Luciferase Buffer (prepared with 1:50 dilution of substrate) and luminescence was measured as described.

### High-throughput imaging assay for parasite and oocyst quantification in growth and drug assays

For drug assays we used either luciferase activity or a 96 well infection and imaging protocol<sup>38</sup> using a BD Pathway instrument. Parasites and host cells were quantified using an ImageJ macro adapted from<sup>39</sup>. The ratio of parasites to host nuclei was determined for each sample image and normalized to untreated controls.

For oocyst quantification by high-throughput microscopy, we weighed collected mouse feces and diluted in PBS (5 µl/mg). Samples were incubated at 95°C for 10 minutes, vortexing every 2 minutes at high speed. Large debris was allowed to settle for 10 min, then 10 µl of the suspension were mixed with 990 µl PBS and 1 µl of FITC conjugated goat polyclonal anti *Cryptosporidium* antibody (GeneTex). After 1 h at RT, the sample was centrifuged at 2000xg for 15 minutes. The pellet was suspended in 200 µl PBS and transferred to a 96-well plate for microscopy. Plates were imaged using BD Pathway and oocysts were counted using an ImageJ macro. Using a standard curve (uninfected mouse feces spiked with known amounts of oocysts) oocyst counts were converted to oocysts per grams feces.

### Quantification of oocyst shedding using quantitative real-time PCR (qRT-PCR)

DNA was extracted from 100 mg feces using ZR Fecal DNA MiniPrep Kit (Zymo Research Corporation, Irvine, CA) following the manufacturer's protocol with slight modification. While in lysis buffer, the sample was freeze-thawed in liquid nitrogen five times prior to the first centrifugation step. Each sample was eluted in 50 µl water, 1 µl of eluate was used for qRT-PCR along with 10 µM primers targeting *Cryptosporidium* 18S rRNA<sup>40</sup> and SYBR Master Mix (Life Technologies, Carlsbad, CA) for detection. Each qRT-PCR reaction was normalized using an 8 point standard curve (fecal DNA purified from uninfected mouse feces spiked with known amounts of oocysts) for each set of samples.

### Oocyst purification from mouse feces

Oocysts were purified from feces using sucrose suspension followed by a cesium chloride centrifugation<sup>41</sup>. Mouse feces were suspended in tap water, passed through a 850 µm mesh filter, followed by 250 µm mesh. This filtered suspension was mixed 1:1 with aqueous sucrose solution (specific gravity 1.33), and centrifuged at 1000xg for 5 min. Oocysts were collected from the supernatant and suspended in 0.85% saline solution. 0.5 ml of this preparation were overlayed onto 0.8 ml of 1.15 specific gravity CsCl, centrifuged for 3 min at 16,000xg. Oocysts were collected from the top ml of the sample, washed in 0.85% saline, counted with disposable counting chamber (KOVA International, Garden Grove, CA) and suspended in 2.5% potassium dichromate for storage at 4°C.

### Western blotting

For Western blot analysis, oocysts from wildtype and transgenic Nlu-Neo were excysted as described above and sporozoites were lysed in SDS sample buffer. Protein extract from 10<sup>7</sup> sporozoites was loaded per lane and subjected to electrophoresis on a precast Any kD Mini-PROTEAN TGX gel (Bio-Rad, Hercules, CA) followed by transfer to 0.2 µm nitrocellulose membrane (Bio-Rad, Hercules, CA). Blots were blocked and probed with an anti-neomycin phosphotransferase II antibody (EMD Millipore, Temecula, CA) at 1:1000 dilution and goat anti-rabbit IgG (H + L)-HRP conjugate (Bio-Rad, Hercules, CA) at 1:20,000 dilution followed by detection with ECL Western Blotting Substrate (Thermo Pierce, Rockford, IL) and exposure to film. Equal loading of blots was controlled by stripping and reprobing with an antibody to αtubulin.

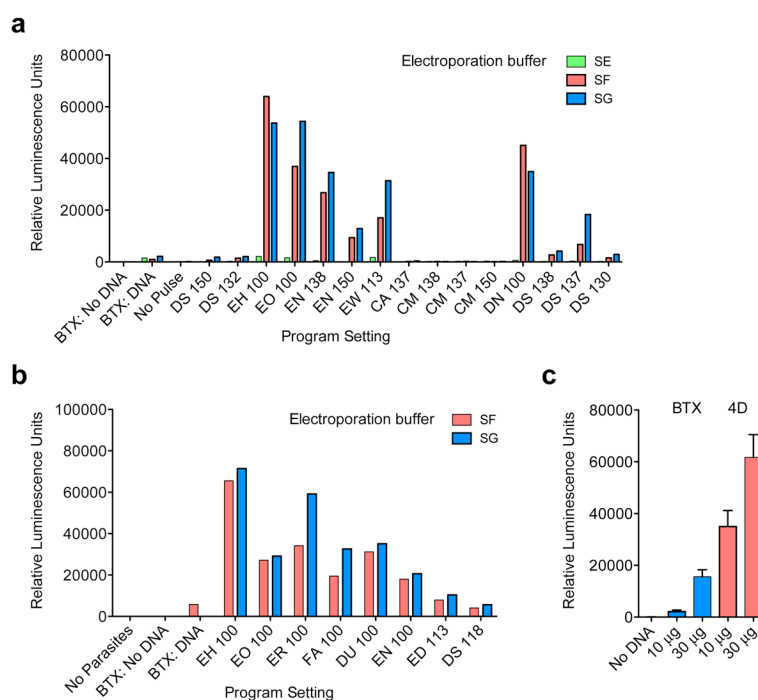
### EdU labeling and immunofluorescence microscopy

5-ethynyl-2'-deoxyuridine (EdU) labeling was performed using the Click-iT EdU Alexa Fluor 594 Imaging Kit following the manufacturer's instructions (Life Technologies, Carlsbad, CA). Purified stable transgenic oocysts expressing the luciferase or wildtype oocysts were inoculated into 24-well plates containing coverslips confluent with HCT-8 cells. After 24 hours, EdU was added to the media at 10  $\mu$ M and left for 18 hours prior to fixation. For immunofluorescence, primary antibodies used were mouse monoclonal anti-human neomycin phosphotransferase II (NPII) (Alpha Diagnostic International Inc., San Antonio, TX), rabbit polyclonal anti-Nanoluciferase antibody (Promega Corporation, Madison, WI), and polyclonal rabbit anti *C. parvum* tryptophan synthase B (TrpB, unpublished) at 1:1000, secondary antibodies were anti-mouse or anti-rabbit conjugated to Alexa488 or Alexa546 (Molecular Probes, Life Technologies, NY) at a dilution of 1:1000. DNA was visualized with DAPI (2 mg/ml). Images were collected on an Applied Precision Delta Vision inverted epifluorescence microscope at the UGA Biomedical Microscopy Core, deconvolved and adjusted for contrast using SoftWoRx software.

### Statistical Methods

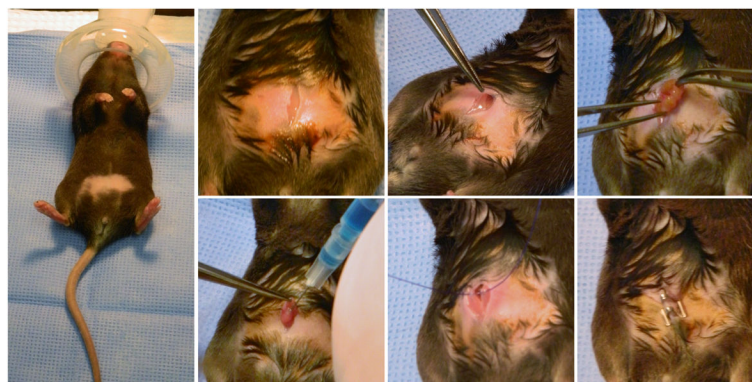
All bar graphs depict the mean with standard deviations shown as error bar. Unless indicated otherwise, graphed data represent three technical replicates; each experiment was repeated at least twice and representative data is shown. No statistical tests were used to predetermine sample size. Unpaired t tests were used appropriately to determine statistical significance and p-value < 0.05 was considered significant. Assumptions for statistical tests were confirmed or corrected as described. No animals were excluded from experimental measurements.

## Extended Data



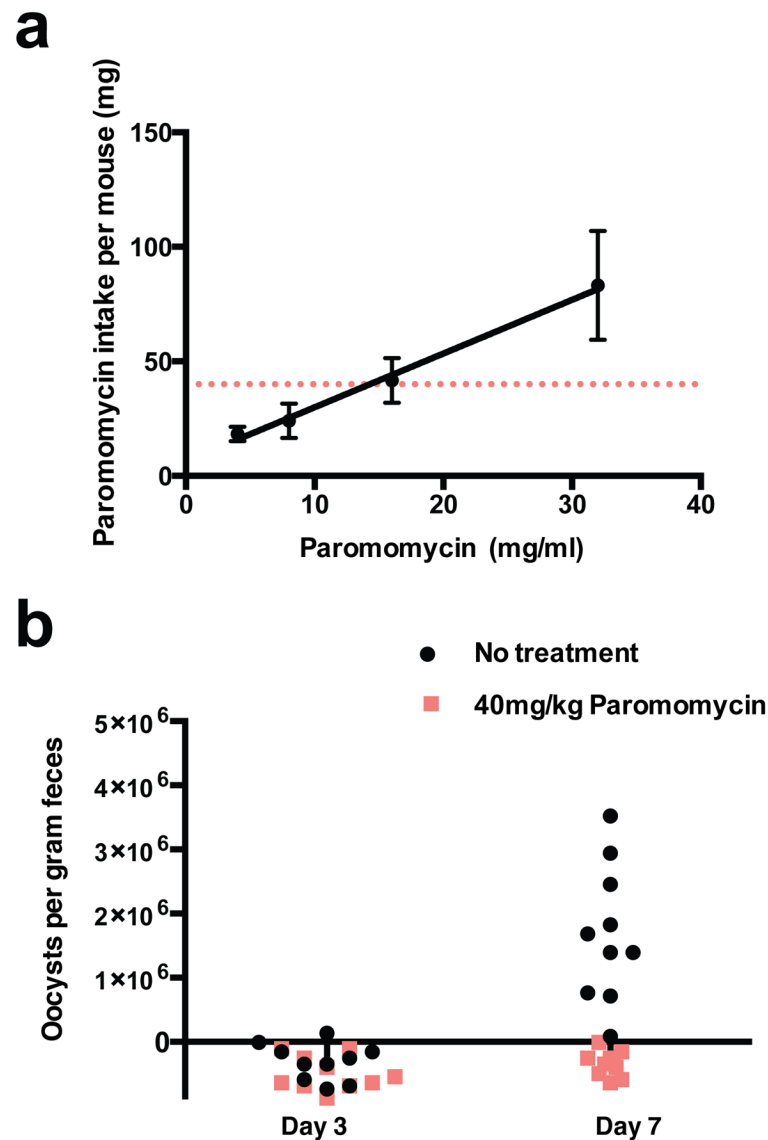
### Extended Data Figure 1. Optimization of sporozoite transfection

**a**, 10 million sporozoites prepared in either cytomix (BTX) or Lonza Buffers SE, SF, or SG (4D Nucleofection) were combined with 10 µg DNA (**Eno\_Nluc-GS-Nluc\_Eno**). Samples were electroporated using previously determined settings for BTX (1500 V, 25 Ω, 25 µF) or various program settings for 4D Nucleofection as indicated. Parasites were added to cultures of HCT-8 cells and luciferase activity was read after 48 hrs. Bars represent average of 2 technical replicates. **b**, Transfection was further optimized by comparing the best preliminary settings (Buffers SF and SG; programs EH 100 and EO 100) with additional pulse programs as indicated. Transfection was carried out as in **a**. Bars represent average of 2 technical replicates. **c**, Electroporation systems (BTX and 4D Nucleofection) were compared using the same number of *C. parvum* sporozoites and quantities of DNA using buffers and conditions optimized in **a** and **b**. Bars represent average of three technical replicates. Note about tenfold enhancement of transient transfection using 4D Nucleofection. The impact of electroporation on stable transformation cannot be assessed in this setup and may be higher. Experiments in **a** and **b** were done once for the purpose of optimization, while **c** was repeated three times, a single representative experiment is shown.



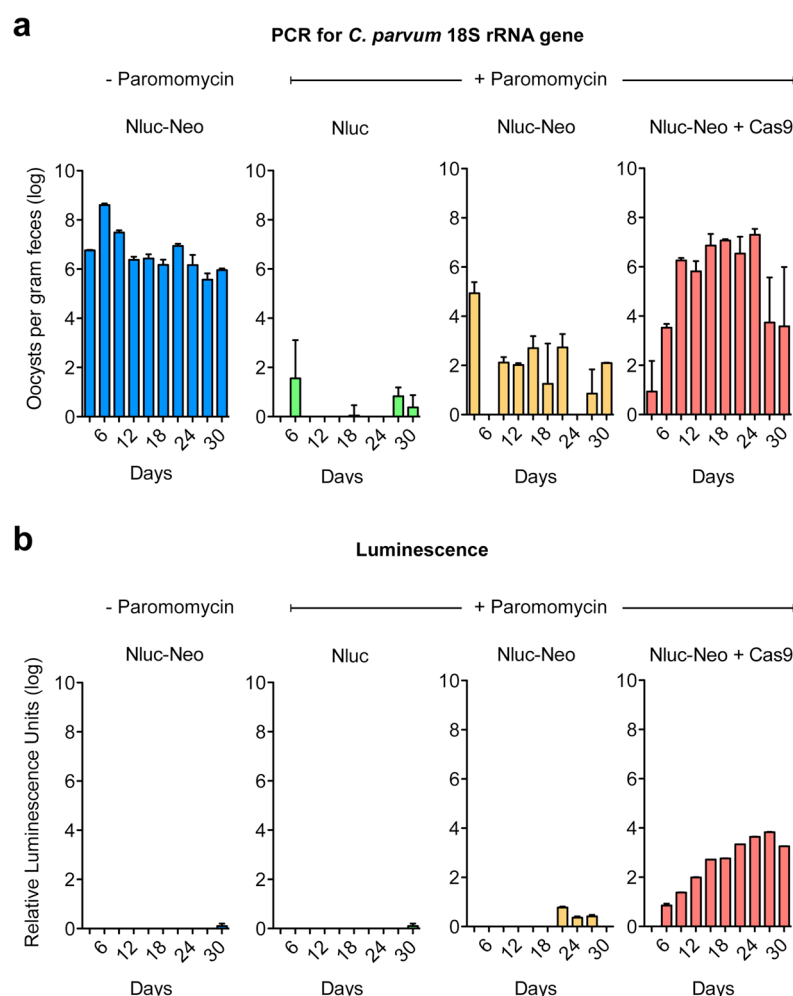
**Extended Data Figure 2. Direct surgical injection of transfected *C. parvum* sporozoites into the small intestine**

Mice are shaved and anaesthetized with isofluorane (3% initially, then maintained at 1.5% for the surgery). The abdominal skin is disinfected with Betadine and a small incision is made into the peritoneum. Forceps are used to grasp the small intestine and 100ul of PBS containing  $10^7$  transfected *C. parvum* sporozoites is injected into the lumen. The peritoneum and the abdominal skin are each sutured with 4-0 polydioxanone and mice are injected with meloxicam (1mg/kg) subcutaneously. Each procedure takes around 15 minutes, and mice recover rapidly.



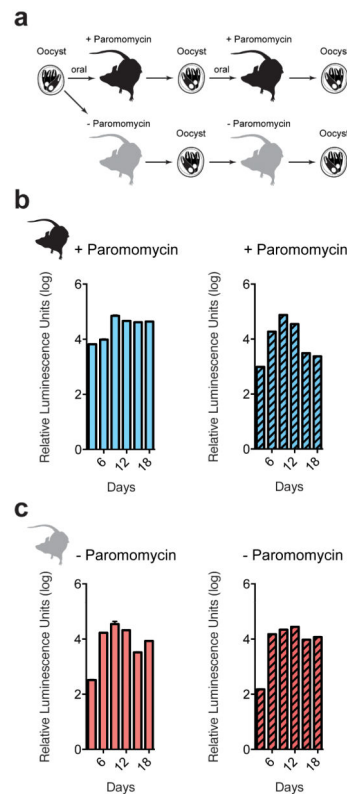
**Extended Data Figure 3. Optimization of paromomycin treatment of infected mice**

**a**, Dosing of mice accounting for drug concentration, animal weight, and measured daily water consumption. At 16mg/ml each mouse received 40mg paromomycin daily (dotted line). **b**, This dose was found to be sufficient to decrease oocyst shedding in treated mice to background. By day 7 mice without paromomycin treatment shed large amounts of oocysts when compared to untreated mice. Treated mice showed no shedding above background. Oocysts were enumerated by high throughput imaging assay. Five mice were analysed individually with two technical replicates.



**Extended Data Figure 4. Mouse model for selection of stable *C. parvum* transgenics**

Repeat of the experiment described in Fig. 3b. **a**, Measurement of *C. parvum* infection using fecal PCR. **b**, Luminescence measurements. Note increasing luminescence from day 6 in parasites that received resistance and Cas9 plasmids. Mice were infected in groups of 4 per cage and pooled feces was analysed for each cage (each measurement represents 3 technical replicates).



### Extended Data Figure 5. *C. parvum* maintains stable transgene when passed serially in mice without paromomycin treatment

**a.** Mice were infected orally with 100,000 transgenic oocysts. Infected mice were then treated with paromomycin (**b**) or left untreated (**c**). Oocysts were purified from fecal collections by sucrose flotation and CsCl centrifugation, and used to infect a second cohort of mice. Again, each mouse received 100,000 transgenic oocysts and mice were treated or not. Feces were tested for luminescence every 3 days. Each reading represents the pooled fecal sample from 5 mice with three technical replicates.

## Supplementary Material

Refer to Web version on PubMed Central for supplementary material.

## Acknowledgments

We thank Lisa Sharling for initial contributions and Liz Hedstrom, Jan Mead, Shipra Vaishnav, Lihua Xiao, and Yasmine Belkaid for discussion. This work was funded in part by the National Institutes of Health (R01AI112427) to BS and a pilot grant from the Centers for Disease Control and the University of Georgia Research Foundation to BS and Lihua Xiao. MJC was supported by training grant NIH T32AI060546 and BS is a Georgia Research Alliance Distinguished Investigator.

## References

1. Kotloff KL, et al. Burden and aetiology of diarrhoeal disease in infants and young children in developing countries (the Global Enteric Multicenter Study, GEMS): a prospective, case-control study. *Lancet*. 2013; 382:209–222.10.1016/S0140-6736(13)60844-2 [PubMed: 23680352]

2. Mondal D, et al. Contribution of enteric infection, altered intestinal barrier function, and maternal malnutrition to infant malnutrition in Bangladesh. *Clin Infect Dis*. 2012; 54:185–192.10.1093/cid/cir807 [PubMed: 22109945]
3. Checkley W, et al. A review of the global burden, novel diagnostics, therapeutics, and vaccine targets for cryptosporidium. *The Lancet Infectious Diseases*. 2014; 10.1016/s1473-3099(14)70772-8
4. Liu L, et al. Global, regional, and national causes of child mortality: an updated systematic analysis for 2010 with time trends since 2000. *Lancet*. 2012; 379:2151–2161.10.1016/S0140-6736(12)60560-1 [PubMed: 22579125]
5. Raja K, et al. Prevalence of cryptosporidiosis in renal transplant recipients presenting with acute diarrhea at a single center in Pakistan. *Journal of nephropathology*. 2014; 3:127–131.10.12860/jnp.2014.25 [PubMed: 25374881]
6. Hunter PR, Nichols G. Epidemiology and clinical features of *Cryptosporidium* infection in immunocompromised patients. *Clin Microbiol Rev*. 2002; 15:145–154. [PubMed: 11781272]
7. Amadi B, et al. Effect of nitazoxanide on morbidity and mortality in Zambian children with cryptosporidiosis: a randomised controlled trial. *Lancet*. 2002; 360:1375–1380. [PubMed: 12423984]
8. Amadi B, et al. High dose prolonged treatment with nitazoxanide is not effective for cryptosporidiosis in HIV positive Zambian children: a randomised controlled trial. *BMC infectious diseases*. 2009; 9:195.10.1186/1471-2334-9-195 [PubMed: 19954529]
9. Striepen B. Parasitic infections: Time to tackle cryptosporidiosis. *Nature*. 2013; 503:189–191. [PubMed: 24236315]
10. Upton SJ, Tilley M, Brillhart DB. Comparative development of *Cryptosporidium parvum* (Apicomplexa) in 11 continuous host cell lines. *FEMS Microbiol Lett*. 1994; 118:233–236. [PubMed: 8020747]
11. Gut J, Nelson RG. *Cryptosporidium parvum*: synchronized excystation in vitro and evaluation of sporozoite infectivity with a new lectin-based assay. *J Eukaryot Microbiol*. 1999; 46:56S–57S. [PubMed: 10519247]
12. Hall MP, et al. Engineered luciferase reporter from a deep sea shrimp utilizing a novel imidazopyrazinone substrate. *ACS chemical biology*. 2012; 7:1848–1857.10.1021/cb3002478 [PubMed: 22894855]
13. Abrahamsen MS, et al. Complete genome sequence of the apicomplexan, *Cryptosporidium parvum*. *Science*. 2004; 304:441–445. [PubMed: 15044751]
14. Theodos CM, Griffiths JK, D'Onfro J, Fairfield A, Tzipori S. Efficacy of nitazoxanide against *Cryptosporidium parvum* in cell culture and in animal models. *Antimicrob Agents Ch*. 1998; 42:1959–1965.
15. Mochizuki K. High efficiency transformation of *Tetrahymena* using a codon-optimized neomycin resistance gene. *Gene*. 2008; 425:79–83.10.1016/J.Gene.2008.08.007 [PubMed: 18775482]
16. Gueirosfilho FJ, Beverley SM. On the Introduction of Genetically-Modified *Leishmania* Outside the Laboratory. *Experimental Parasitology*. 1994; 78:425–428.10.1006/expr.1994.1048 [PubMed: 8206143]
17. Fox BA, Ristuccia JG, Gigley JP, Bzik DJ. Efficient gene replacements in *Toxoplasma gondii* strains deficient for nonhomologous end-joining. *Eukaryot Cell*. 2009 EC.00357-08 [pii]. 10.1128/EC.00357-08
18. Lee AH, Symington LS, Fidock DA. DNA repair mechanisms and their biological roles in the malaria parasite *Plasmodium falciparum*. *Microbiol Mol Biol Rev*. 2014; 78:469–486.10.1128/MMBR.00059-13 [PubMed: 25184562]
19. Brooks CF, et al. The *Toxoplasma* apicoplast phosphate translocator links cytosolic and apicoplast metabolism and is essential for parasite survival. *Cell Host Microbe*. 2010; 7:62–73. S1931-3128(09)00412-0 [pii] . 10.1016/j.chom.2009.12.002 [PubMed: 20036630]
20. Jinek M, et al. A programmable dual-RNA-guided DNA endonuclease in adaptive bacterial immunity. 2012; 337:816–821.10.1126/science.1225829
21. Sidik SM, Hackett CG, Tran F, Westwood NJ, Lourido S. Efficient Genome Engineering of *Toxoplasma gondii* Using CRISPR/Cas9. *Plos One*. 2014; 9 ARTN e100450. 10.1371/journal.pone.0100450

22. Griffiths JK, Theodos C, Paris M, Tzipori S. The gamma interferon gene knockout mouse: a highly sensitive model for evaluation of therapeutic agents against *Cryptosporidium parvum*. *J Clin Microbiol*. 1998; 36:2503–2508. [PubMed: 9705383]
23. Fayer R, Nerad T, Rall W, Lindsay DS, Blagburn BL. Studies on Cryopreservation of *Cryptosporidium-Parvum*. *Journal of Parasitology*. 1991; 77:357–361.10.2307/3283119 [PubMed: 2040948]
24. Liu JY, Bolstad DB, Bolstad ESD, Wright DL, Anderson AC. Towards New Antifolates Targeting Eukaryotic Opportunistic Infections. *Eukaryotic Cell*. 2009; 8:483–486.10.1128/Ec.00298-08 [PubMed: 19168759]
25. Striepen B, et al. Gene transfer in the evolution of parasite nucleotide biosynthesis. *Proc Natl Acad Sci U S A*. 2004; 101:3154–3159. 0304686101 [pii]. 10.1073/pnas.0304686101 [PubMed: 14973196]
26. Salic A, Mitchison TJ. A chemical method for fast and sensitive detection of DNA synthesis in vivo. *P Natl Acad Sci USA*. 2008; 105:2415–2420.10.1073/Pnas.0712168105
27. Striepen, B. Antimicrobial Drug resistance. Mayers, DL.; Lerner, SA.; Ouellette, M.; Sobel, JD., editors. Vol. 1. Springer; 2009. p. 605-621.
28. Sheoran A, Wiffin A, Widmer G, Singh P, Tzipori S. Infection with *Cryptosporidium hominis* provides incomplete protection of the host against *Cryptosporidium parvum*. *J Infect Dis*. 2012; 205:1019–1023.10.1093/infdis/jir874 [PubMed: 22279124]
29. McDonald V, Deer R, Uni S, Iseki M, Bancroft GJ. Immune responses to *Cryptosporidium muris* and *Cryptosporidium parvum* in adult immunocompetent or immunocompromised (nude and SCID) mice. *Infect Immun*. 1992; 60:3325–3331. [PubMed: 1639500]
30. Jiang L, Lee PC, White J, Rathod PK. Potent and selective activity of a combination of thymidine and 1843U89, a folate-based thymidylate synthase inhibitor, against *Plasmodium falciparum*. *Antimicrob Agents Ch*. 2000; 44:1047–1050.10.1128/Aac.44.4.1047-1050.2000
31. Harb OS, Roos DS. The Eukaryotic Pathogen Databases: A Functional Genomic Resource Integrating Data from Human and Veterinary Parasites. *Parasite Genomics Protocols*, Second Edition. 2015; 1201:1–18.10.1007/978-1-4939-1438-8\_
32. van Dooren GG, Tomova C, Agrawal S, Humbel BM, Striepen B. *Toxoplasma gondii* Tic20 is essential for apicoplast protein import. *Proc Natl Acad Sci U S A*. 2008; 105:13574–13579. [PubMed: 18757752]
33. Gubbels MJ, Li C, Striepen B. High-Throughput Growth Assay for *Toxoplasma gondii* Using Yellow Fluorescent Protein. *Antimicrob Agents Chemother*. 2003; 47:309–316. [PubMed: 12499207]
34. Saeij JP, Boyle JP, Grigg ME, Arrizabalaga G, Boothroyd JC. Bioluminescence imaging of *Toxoplasma gondii* infection in living mice reveals dramatic differences between strains. *Infect Immun*. 2005; 73:695–702. [PubMed: 15664907]
35. Cong L, et al. Multiplex genome engineering using CRISPR/Cas systems. 2013; 339:819–823.10.1126/science.1231143
36. Chakrabarti K, et al. Structural RNAs of known and unknown function identified in malaria parasites by comparative genomics and RNA analysis. *RNA*. 2007; 13:1923–1939.10.1261/rna.751807 [PubMed: 17901154]
37. Striepen, B.; Soldati, D. *Toxoplasma gondii*: The Model Apicomplexan - Perspective and Methods. Weiss, LM.; Kim, K., editors. Elsevier; 2007. p. 391-415.
38. Sharling L, et al. A screening pipeline for antiparasitic agents targeting cryptosporidium inosine monophosphate dehydrogenase. *PLoS neglected tropical diseases*. 2010; 4:e794.10.1371/journal.pntd.0000794 [PubMed: 20706578]
39. Bessoff K, Sateriale A, Lee KK, Huston CD. Drug repurposing screen reveals FDA-approved inhibitors of human HMG-CoA reductase and isoprenoid synthesis that block *Cryptosporidium parvum* growth. *Antimicrob Agents Chemother*. 2013; 57:1804–1814.10.1128/AAC.02460-12 [PubMed: 23380723]
40. Mary C, et al. Multicentric Evaluation of a New Real-Time PCR Assay for Quantification of *Cryptosporidium* spp. and Identification of *Cryptosporidium parvum* and *Cryptosporidium*

- hominis. *Journal of Clinical Microbiology*. 2013; 51:2556–2563.10.1128/Jcm.03458-12 [PubMed: 23720792]
41. Upton, SJ. *Cryptosporidium and Cryptosporidiosis*. Fayer, R., editor. CRC Press; 1997. p. 181-207.

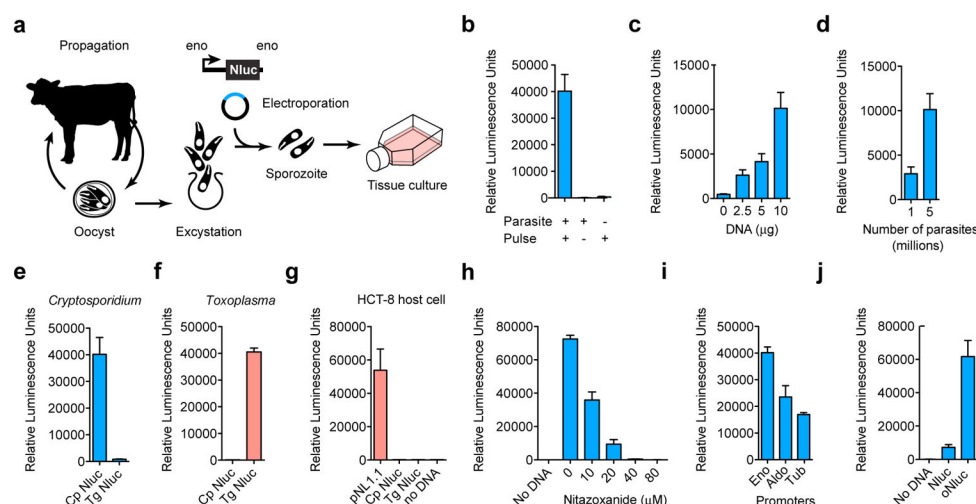


**Figure 1. Transfection of *Cryptosporidium parvum***

**a.** Schematic overview. *C. parvum* sporozoites were prepared from oocysts purified from infected calves and electroporated in the presence of plasmid DNA prior to infection of HCT-8 cells. Luminescence measurements (the means of 3 technical replicates, s.d. shown as error bar) of *T. gondii* (f), human HCT-8 cells (g), or *C. parvum* (all other panels, blue) transfected with nanoluciferase (Nluc) expression plasmids. *C. parvum* transfection requires electroporation (b) of DNA (c) into parasites (d). Transfection also requires plasmids to carry parasite specific promoter sequences (e, f, testing *C. parvum* and *T. gondii* promoters in both parasites), and is susceptible to the *Cryptosporidium* drug nitazoxanide (h). Lipofection of HCT-8 cells with the original Nluc plasmid pNL1.1 (Promega), but not derived parasite vectors results in luciferase activity in the host alone (g). Choice of promoter (i, Eno, enolase; Aldo, aldolase; Tub, alpha-tubulin 5' regions, the 3' UTR was uniformly from the enolase gene) or codon composition (j, oNluc, optimized to 35% GC) influences expression level in *C. parvum*. Note automatic gain adjustment of luminescence measurements, units are not comparable between panels. Independent experiments were repeated 3 times, and representative data are shown.

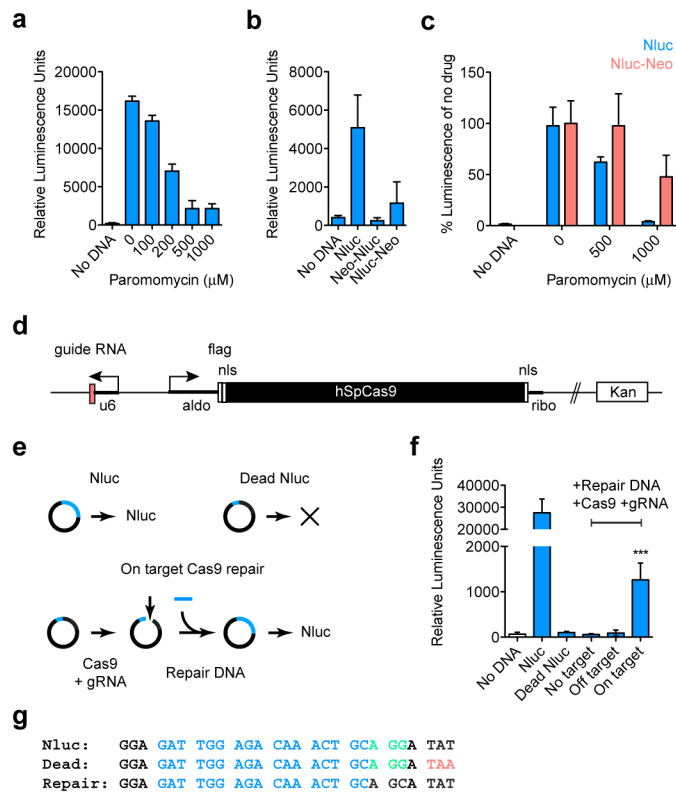
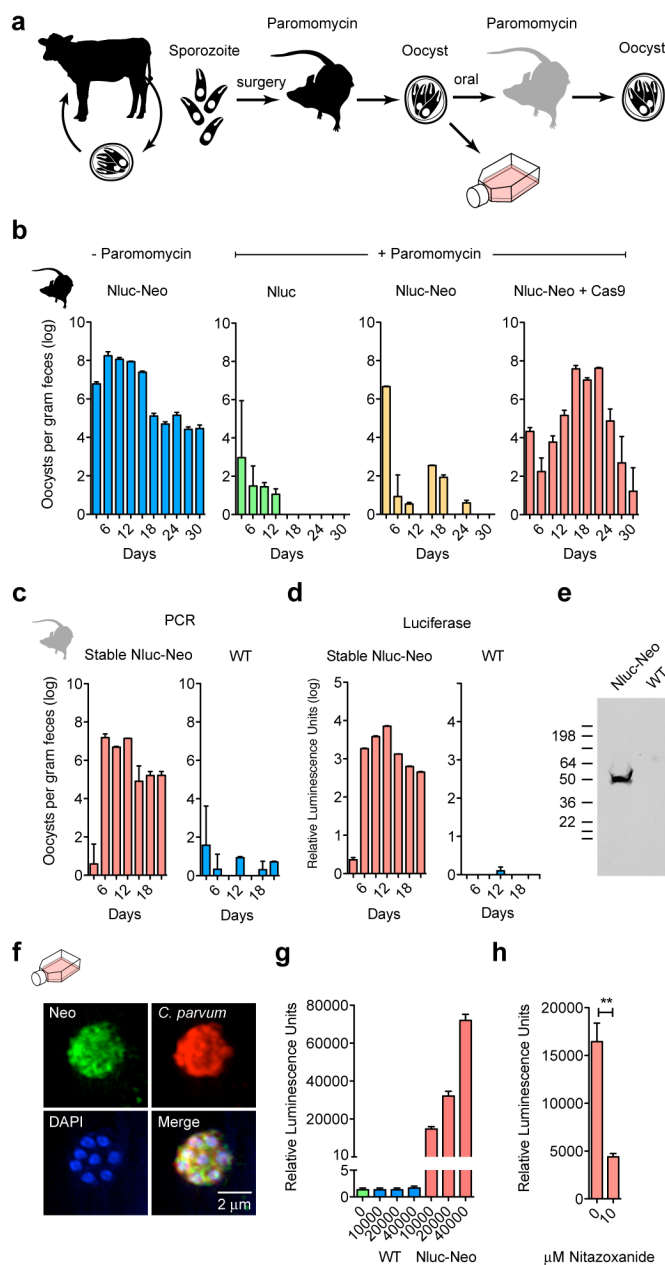


**Figure 2. Luciferase assays for *C. parvum* drug resistance and CRISPR/Cas9 activity**

**a**, HCT-8 cells were infected with Nluc transfected sporozoites and grown for 2 days in presence of paromomycin. **b**, Translational fusions were constructed placing Neo to the N- or C-terminus of Nluc. Nluc-Neo shows luciferase activity, albeit at reduced level when compared to Nluc alone. **c**, *C. parvum* transfected with Nluc (blue) or Nluc-Neo (red) were grown in different concentrations of paromomycin. Luciferase activity for each plasmid was normalized to its drug free level. **d**, CRISPR/Cas9 plasmid for *C. parvum* (u6, newly annotated promoter CM000433:553110–553472; nls, nuclear localization signal; flag, epitope tag; ribo, ribosomal protein L13a 3' UTR). **e**, Outline and **g**, sequences for Nluc repair assay (guide RNA target, blue; protospacer adjacent motif, green; mutagenized codon 18, red). **f**, Sporozoites were transfected with Nluc or a codon 18 termination mutant (Dead Nluc), note ablation of signal. In addition to the Dead Nluc plasmid, some parasites also received a 125 bp double-stranded repair DNA fragment, and the Cas9 plasmid with the indicated guide RNAs (no target, empty gRNA cassette; off target, GFP gRNA; on target, Nluc gRNA). Statistical analysis compares Dead Nluc alone with Dead Nluc and Cas9 and specific gRNA. Note significant Cas9 mediated restoration of luciferase activity (\*\*\*) $p=0.0006$ , unpaired *t* test).  $n=3$  technical replicates for **a**, **b**, **c**, and controls from **f**;  $n=6$  technical replicates for On target samples in **f**. Error bar is s.d. and all experiments depicted here were repeated 3 times and representative data are shown.



**a**, Outline. Transfected sporozoites were injected into the small intestine by surgery (Extended Data Fig. 2) and mice were treated with paromomycin. Oocysts were purified from the feces and used to infect cultures or mice by oral gavage. **b**, Quantitative PCR of *C. parvum* DNA isolated from feces of mice infected with transfected sporozoites (four mice per group) and treated as indicated. Emergence of paromomycin resistance required **Nluc-Neo** and a **Cas9** plasmid. Upon reinfection parasites show strong drug resistance (**c**) and luciferase activity (**d**). In repeat experiments we noted that luciferase is detectable as early as 6 days after transfection in the feces of the first infected mouse (Extended Data Fig. 4). **e**, Protein extracts from oocysts were analysed by SDS-PAGE and Western blot using an

antibody against Neo (rabbit anti-neomycin phosphotransferase II, EMD Millipore). Predicted molecular mass of the Nluc-Neo fusion protein is 48.3 kDa. **f**, Immunofluorescence staining using anti Neo (mouse anti Neo, Alpha Diagnostic Inc.) and *C. parvum* (tryptophan synthase B) antibodies. Note multiple nuclei in DAPI stain typical for *C. parvum* meronts. No anti Neo staining was observed in wild type parasites. **g**, Luciferase assays for HCT-8 cultures infected with wild type (WT, blue) and transgenic (Nluc-Neo, red) parasites. Y-axis is split to show level of background. n=3 technical replicates, error bar is s.d., experiment done twice. **h**, 96-well luciferase drug assay using 1000 oocysts per well. Note significant growth inhibition on treatment with 10  $\mu$ M nitazoxanide (\*\*p=0.0036, unpaired *t* test). n=3 technical replicates, error bar is s.d., experiment was repeated two times and representative data are shown.

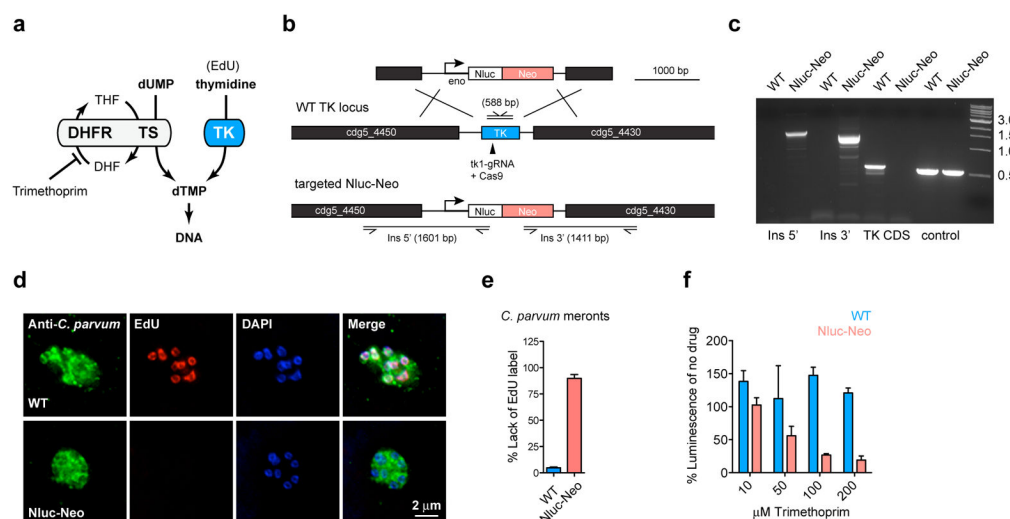


**Figure 4. Targeted deletion of *C. parvum* thymidine kinase**

**a**, Due to a horizontal gene transfer *C. parvum* has two pathways to synthesize dTMP: thymidine kinase (TK) and dihydrofolate reductase-thymidylate synthase (DHFR-TS). DHF and THF, dihydro- and tetrahydrofolic acid. **b**, Map of the *C. parvum* TK locus, the targeting plasmid and the predicted modified locus. Primers and amplicon sizes of diagnostic PCR products are indicated. **c**, PCR analysis using genomic DNA from wild type (WT) and transgenic parasites (Nluc-Neo, oocysts purified from feces of infected mice shown in Fig. 3c). Primer sequences are provided in a Table S1 in the supplementary material. **e**, Quantification of EdU labelling experiments (meronts with 4 or more nuclei were scored, two biological repeats, n=105 each sample, error bar is s.d.), **d** shows representative fluorescence micrographs. Antibody to *C. parvum* tryptophan synthase B was used to identify parasites (green). **f**, Trimethoprim treatment of WT (blue) and Nluc-Neo transgenic (red) parasites. WT parasites were measured in transient transfection assays with Nluc plasmid (n=3, technical replicates, error bar is s.d.). Assay shown was conducted in the presence of 10  $\mu$ M thymidine to avoid indirect host cell toxicity<sup>30</sup> (experiments without thymidine produced indistinguishable results). Experiments were repeated 3 times and representative data are shown.